JCI insight

MG53 suppresses NFκB activation to mitigate age-related heart failure

Xiaoliang Wang, … , Chuanxi Cai, Jianjie Ma

JCI Insight. 2021. https://doi.org/10.1172/jci.insight.148375.

Research In-Press Preview Aging Cardiology

Graphical abstract

Graphical abstract: Long-term administration of rhMG53 suppresses NFκB activation to mitigate age-related heart failure.

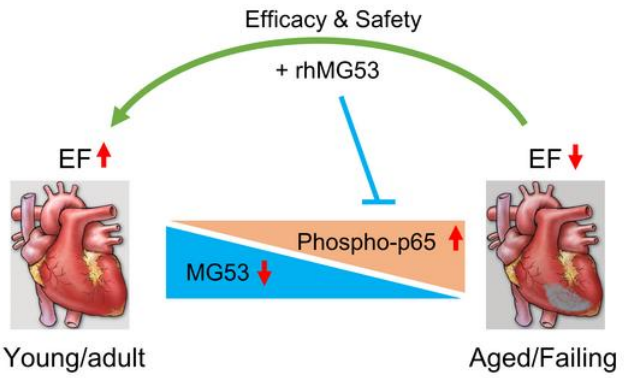

MG53 suppresses NFκB activation to mitigate age-related heart failure

Xiaoliang Wang[1], Xiuchun Li[1], Hannah Ong[1], Tao Tan[1,2], Ki Ho Park[1], Zehua Bian[1], Xunchang Zou[3], Erin Haggard[1], Paul Janssen[4], Robert E. Merritt[1], Timothy M. Pawlik[1], Bryan A. Whitson[1], Nahush A. Mokadam[1], Lei Cao[3], Hua Zhu[1], Chuanxi Cai[1,*], and Jianjie Ma[1,2*]

[1] Department of Surgery, Division of Cardiac Surgery, Davis Heart and Lung Research Institute, The Ohio State University, Columbus, OH 43210

[2] TRIM-edicine, Inc., 1275 Kinnear Road, Columbus, OH 43212

[3] Department of Cancer Biology and Genetics, College of Medicine, The Ohio State University, Columbus, OH 43210

[4] Department of Physiology and Cell Biology, Davis Heart and Lung Research Institute, The Ohio State University, Columbus, OH 43210

[*] Corresponding authors:

Jianjie Ma, PhD, 614-292-2636, Jianjie.Ma@osumc.edu

Chuanxi Cai, PhD, 614-292-2213, Chuanxi.Cai@osumc.edu

Declaration of Conflicts of Interest

J.M. and T.T. hold equity interest in TRIM-edicine, Inc., a university spin-off biotechnology company that develops MG53 for regenerative medicine application. Rutgers University and Ohio State University own the Intellectual property related to MG53.

Abstract

Aging is associated with chronic oxidative stress and inflammation that impact the tissue repair and regeneration capacity. MG53 is a TRIM family protein that facilitates repair of cell membrane injury in a redox-dependent manner. Here we demonstrate that the expression of MG53 is reduced in failing human heart and aging mouse heart, concomitant with elevated NFκB activation. We evaluate the safety and efficacy of longitudinal, systemic administration of recombinant human MG53 (rhMG53) protein in aged mice. Echocardiography and pressure-volume loop measurements reveal beneficial effects of rhMG53 treatment in improving heart function of aging mice. Biochemical and histological studies demonstrate the cardioprotective effects of rhMG53 are linked to suppression of NFκB-mediated inflammation, reducing apoptotic cell death and oxidative stress in the aged heart. Repetitive administrations of rhMG53 in aged mice do not have adverse effects on major vital organ functions. These findings support the therapeutic value of rhMG53 in treating age-related decline in cardiac function.

Key Words: MG53/TRIM72, aging, heart failure, NFκB, inflammation.

Introduction

Chronic loss of cardiomyocyte integrity underlies human heart failure (HF) associated with aging that often involves progression of acute myocardial infarction (MI) and the maladaptive response of cardiomyopathy (1). During MI, the membrane repair function of cardiomyocytes is compromised, and protection of membrane integrity is an important strategy to treat MI and HF. In addition, chronic oxidative stress and inflammation associated with aging can render the cardiomyocytes more susceptible to stress-induced MI. Therefore, a therapeutic approach that restores tissue integrity and mitigates inflammation can potentially be an effective means to treat age-related organ dysfunction.

We previously identified MG53 as an essential component of cell membrane repair (2-6). MG53 nucleates the assembly of the membrane repair machinery in a redox-dependent manner. Mice without the MG53 gene develop cardiac pathology due to defective membrane repair and increased susceptibility to cardiac injury (7, 8). Transgenic mice with sustained elevation of MG53 in the bloodstream (~100 fold higher circulating MG53 vs wild type mice) lived a healthier and longer lifespan compared with the littermate wild type mice, and displayed increased tissue healing and regeneration capacity following injury (9). While we have demonstrated that intravenous administration of recombinant human MG53 (rhMG53) protein could protect against acute heart injury in rodent and porcine models of ischemia-reperfusion induced MI (5, 10), whether rhMG53 has beneficial effects on chronic HF remains to be determined.

NF-κB is an inflammatory nuclear transcription factor that modulates cardiac function under both physiological and pathophysiological conditions (11, 12). Upregulation of NF-κB is associated with cardiac aging (13), and inhibition of NF-κB signaling in mice displayed beneficial effects for HF, which is related with reduced levels of apoptosis (14) and reactive oxygen species (ROS) production (15-17). Therefore, controlling ROS production has potential benefits to delay aging progression. Moreover, recent studies have revealed important cross talk between inflammation and oxidative stress in the pathogenesis of cardiovascular disease (18, 19). Studies from us and other investigators have suggested

a role for MG53 in control of NF-κB signaling in neuroprotection (20), cardiac hypertrophy (21) and viral infection (22). However, it is not clear how MG53 regulates NF-κB signaling in the aging heart.

In this study, we investigated the expression of MG53 in failing human hearts and aging mouse hearts, and examined whether longitudinal administration of recombinant human MG53 protein in aged mice is safe and exhibits any beneficial effect on the age-related decline of heart function.

Result

Expression of MG53 and NFκB-p65 in failing human hearts and aging mouse heart

Previous study by Lemckert et al reported low levels of MG53 protein in human hearts (23). We used a custom-made high-affinity antibody that recognizes the human MG53 protein (24) and found that the MG53 protein level is remarkably reduced in the failing human hearts compared with the non-failing heart, based on western blotting (**Figure 1A**). Meanwhile, increased levels of phosphorylated NF-κB p65 (p-p65) were observed in failing human hearts versus non-failing human hearts (**Figure 1A** and **1B**). The demographic information of the human patients is provided in the **Table 1**. The strong correlation between reduced expression of MG53 and elevated activation of NF-κB (**Figure 1C**) suggests the possibility that the aging human hearts are pre-disposed to inflammation which may render then more susceptible to stress-induced cardiac injury.

We obtained aged C57BL/6J mice (24 months age) from the rodent consortium of the National Institute on Aging. Echocardiography revealed compromised left-ventricular ejection fraction (EF) in the aging versus young mice (3 months age) of the same genetic background (**Figure 1D**). Similar to the human heart, western blot showed that the protein level of MG53 was considerably lower in aging mouse hearts versus young mouse hearts. While the total amount of NF-κB p65 did not appear to change in the aging mouse heart, the phosphorylated p65 (p-p65) was significantly elevated in the aging mouse hearts compared with the young mouse heart (**Figure 1E** and **1F**).

Systematic administration of rhMG53 mitigates HF in aging mice

We designed a protocol to evaluate the safety and therapeutic potential with longitudinal administration of rhMG53 in the aged mice (**Figure 2A**). A total of sixty C57BL6 mice were examined (24-25 months, 30 male and 30 female). Half of the mice received saline and half received rhMG53 (6 mg/kg, subcutaneous, daily for 6 weeks). The experiment and data analyses were conducted blindly. Repetitive rhMG53 administration did not produce adverse effects in aged animals, as only 1 out of 30

rhMG53-treated mice died during the 6-week treatment, whereas 5 out of 30 mice died in the saline control group (**Figure 2B**). The mouse cardiac function was monitored longitudinally using echocardiography, which revealed progressive improvement in ejection fraction (EF) in animals treated with rhMG53 vs those treated with saline (**Figure 2C**). After 6 weeks of rhMG53 treatment, both male and female mice exhibited significant improvement in EF compared with saline treatment. At the end of the 6 week treatment period, terminal pressure-volume loop (PV-loop) assessment was performed to evaluate the changes in contractile function of the mouse heart. As shown in **Figure 2D**, a clear left-shift of the PV-loop was observed with the aged mice receiving rhMG53 vs saline control, indicating an improvement in heart function. Quantitative analyses of the PV-loop measurement demonstrated significant improvement of EF in aged mice that received the longitudinal rhMG53 treatment (**Figure 2E**).

Longitudinal administration of rhMG53 is cardioprotective in aging mice

Real-time PCR was conducted for cardiac tissue samples collected from the above animal studies to quantify the changes in NF-κB related signaling components. As shown in **Figure 3A**, we found increased gene expression of IFNγ, IL-1β, IL6, and TNFα in the aging mouse hearts (25 months old) compared to the young mouse hearts (3 months old). Following the 6-week rhMG53 treatment, these myocardial inflammatory genes in the aging mouse heart were significantly diminished when compared to those receiving saline as control (**Figure 3A**).

We next conducted biochemical assays to determine the signaling machinery that potentially contributes to the cardioprotective effect of rhMG53 in the aged heart (**Figure 3B-C**). *First*, compared to the young mouse hearts, we found that the elevated levels of p-p65 in aging mouse hearts was significantly reduced by the administration of rhMG53. The cardioprotective effect of rhMG53 appeared to be linked to suppression of NFκB-mediated inflammation in aged mouse heart, where the p-p65/total p65 ratio changed from 4.15±0.35 (+saline) to 2.27±0.34 (+rhMG53) ($p<0.01$, $n=3$). *Second,* we observed that the reduced expression of endogenous MG53 protein in the aging mouse heart was partially restored after the 6-week period of repetitive rhMG53 treatment. Since the western blot was performed at 1 week

after the last rhMG53 administration (when mice were sacrificed and heart isolated), the increased MG53 protein unlikely originated from the exogenous rhMG53. *Third*, we found that the protein expression of IL6 and TNFα, the downstream of NF-κB regulated pro-inflammatory markers, were higher in hearts derived from aged mice receiving saline (which is consistent with other investigators (18, 19)), and rhMG53 treatment ameliorated the elevated expression of IL6 and TNFα in the aging mouse heart (**Figure 3B-C**).

TUNEL staining was performed with sections of the mouse heart to evaluate the potential benefits of rhMG53 in preserving cardiomyocyte integrity in the aged mice. As shown in **Figure 3D-E**, mouse heart with rhMG53 treatment exhibited significantly less TUNEL positive cells versus the saline control group. Overall, these data suggest that the multi-cellular function of rhMG53 in cardioprotection is associated with anti-inflammation and reduced apoptotic cell death in aging heart.

Effects of rhMG53 treatment on oxidative stress response in aging hearts

We also investigated the activity of antioxidant and oxidant proteins in aging mouse heart treated with saline or rhMG53. As shown in **Figure 4A-B,** the protein level for catalase and GPX1, known antioxidant proteins, were significantly lower in saline-treated aged mouse hearts compared with the young mouse hearts, whereas the protein level of NADPH oxidase 4 (NOX4), one of the genes thought be responsible for oxidative stress, was considerably higher in saline-treated aged mouse hearts compared with the young mouse hearts (**Figure 4A-B**). rhMG53 treatment restored the expression of catalase and GPX1, and decreased the expression of NOX4 in the aged mouse hearts. These findings indicated that rhMG53 treatment could reduce oxidative stress in the aged mouse heart.

Dihydroethidium (DHE) fluorescence staining was conducted to determine the level of ROS in the mouse hearts. The DHE fluorescence intensity was lower in young mouse heart (**Fig. 4C**), compared with the aged mouse heart receiving saline treatment (**Fig. 4D**). The aged mice receiving the 6-week longitudinal treatment with rhMG53 showed significant reduction of DHE fluorescent intensity (**Fig. 4E**).

Data from multiple animals were summarized in **Fig. 4F**. Collectively, these data suggest that the longitudinal treatment with rhMG53 suppressed age-induced oxidative stress response in the heart.

Repetitive administration of rhMG53 is safe in aging mice

Over the 6-week rhMG53 treatment period, each mouse would receive a total of ~6 mg rhMG53 protein. If there were any immune response or toxicity with the repetitive rhMG53 administration in the aged mice, this should be reflected in the vital organs, including heart, liver, and spleen. Our previous published data (25) showed that the young, healthy rats treated with repetitive administration of rhMG53 (up to 40 mg/kg), did not show any sign of cardiotoxicity or adverse effects. We did not expect that repetitive rhMG53 administration has any side effects on healthy young mice, thus we did not include a group of young mice treated with rhMG53 in the present study.

After sacrificing the animals at the end point, the heart weight (HW) and tibia length (TL) were measured. The HW/TL ratios of the individual mouse were plotted (**Figure 5A,** *left*)**.** Clearly, there was no changes in HW/TL with or without rhMG53 treatment. Echocardiographic analyses showed no significant differences in diastolic and systolic LV anterior wall thickness or posterior wall thickness in aging mice treated with rhMG53 or saline (**Supplemental Figure S1**), suggesting that repetitive rhMG53 administration did not induce hypertrophy or hypotrophy in the aged mouse heart. Meanwhile, the ratios of the liver weight over the body weight (**Figure 5A**, *middle*) and the spleen weight over the body weight (**Figure 5A**, *right*) did not appear to be different between the mice receiving rhMG53 or saline. We also quantified the serum levels of alanine aminotransferase (ALT), alkaline phosphatase (ALP), and total bilirubin (TBILI) as biomarkers for liver injury and dysfunction as biomarkers for liver injury and dysfunction (**Figure 5B**), and found no significant differences between the two groups of aged mice. Furthermore, the serum contents of high-density lipoprotein (HDL), low density lipoprotein (LDL) and triglycerides were also quantified (**Figure 5C**). Additionally, we quantified the serum levels of lactate dehydrogenase (LDH) and creatine kinase (CK), and found no significant difference between the saline control and rhMG53 treatment groups (**Figure 5D**). Overall, there were no measurable changes in ALT,

ALP, total bilirubin, LDL, HDL, triglycerides, LDH, and CK in aged mice following the 6-week treatment with rhMG53, suggesting no adverse effects of rhMG53 on hepatic and cardiovascular functions. These data support the safety for systemic and repetitive rhMG53 administration in aged mice.

Discussion

Elderly people have an increased risk for myocardial infarction and heart failure due to compromised tissue repair and regeneration. In this study, we show that the expression of MG53 is decreased in both the failing human heart and the aging mouse heart, which is accompanied by elevation of NFκB activation. Longitudinal administration of rhMG53 mitigated the heart dysfunction in the aged mice. We demonstrate that repetitive rhMG53 administration in aged mice is safe and effective in reducing apoptotic cardiomyocyte death and suppressing the chronic inflammation mediated by NFκB. These findings may provide a basis for the potential use of rhMG53 to treat aging related HF.

Since our initial discovery of MG53 in 2009, notable progress has been made in advancing the mechanistic action of this gene in the biology of tissue repair as well as the regulation of metabolic syndromes. We know that genetic ablation of MG53 leads to defective cell membrane repair, which can cause progressive skeletal myopathy (2) and reduced survival capacity of cardiomyocytes (7). We recently reported that transgenic mice (tPA-MG53) with sustained elevation of MG53 in the bloodstream lived a healthy life-span and displayed enhanced tissue regenerative capacity without impairing the body's metabolic function of glucose handling and insulin signaling (9). In the present study, we demonstrated for the first time rhMG53 has anti-aging function, e.g., systemic administration of the rhMG53 protein improves survival of the aging mice. We present *in vivo* data to show that rhMG53 is effective and safe in preventing age-related heart failure. Our results demonstrated that the aging mice at the end-stage of their life (25-27 months age) could tolerate repetitive systemic administration of rhMG53 (6 mg/kg) on a daily basis for 6 weeks. Using a combination of human data and biochemical analyses, we presented evidences that the therapeutic benefit of rhMG53 is linked to mitigation of aging-related inflammation and oxidative stress.

Xiao and colleagues proposed that MG53-mediated downregulation of IRS-1 could serve as a causative factor for the development of type II diabetes(26), but early studies from other investigators demonstrated that genetic ablation of IRS-1 is not sufficient to induce type II diabetes in mice(27, 28).

Wu et al. recently reported an immuno-approach using MG53 antibody could reduce serum glucose to treat diabetes(29) (see also Zhu et al(30), letter to *Circulation* editor). We have obtained a substantial amount of data establishing the safety profile of systemic rhMG53 delivery in rodents (31-34), pigs (5), and dogs (33). In particular, the pharmacokinetic properties for rhMG53 in the serum remained unchanged between the beginning and the end of repeated intravenous dosing in dogs (33), suggesting that systemic administration of the human MG53 protein does not produce anti-drug antibody response in dogs. Data presented in this study further showed that long-term repetitive dosing of rhMG53 is safe and did not alter the liver and cardiovascular function of aged mice.

Increased oxidative stress and apoptosis were associated with the pathogenesis of heart failure in aging (16, 17). Free radicals generated by reactive oxygen species are maintained at physiological levels by several endogenous antioxidants, including catalase. Previous study demonstrated that cardiac aging phenotypes were significantly ameliorated by overexpression catalase in a murine model (16). Over production of reactive oxygen species in aging is known to trigger NFκB-related inflammatory signaling in cardiomyocytes (12, 13, 15). Our results demonstrated that aging significantly increased NFκB-mediated inflammatory response, and decreased the expression of anti-oxidant proteins in heart tissue, which were partially recovered by the long-term administration of rhMG53, leading to reduced cardiac inflammation, ROS production, and cardiac apoptosis.

We were surprised to see the decreased total p65 protein in failing human hearts vs non-failing age matched human hearts (as shown in Fig. 1A). A previous study by Morishita et al using an NF-κB binding decoy oligonucleotide to down-regulate p65 expression in the rat heart demonstrated that reduced p65 expression had benefits in reducing myocardial infarction following coronary artery ligation (35). It is possible that decreased total p65 expression might be associated with the adaptation of the progression of heart failure. Further studies are required to test this possibility.

Some previous studies showed healthy aged mice did not exhibit significant systolic dysfunction rather than impaired diastolic function. However, most of these studies used mice with relative younger

age, including mice at age of 6-18 months (36), 18-19 months (37, 38), or 20-24 months (39). However, the mice used in our present study were 24-25 months age at the start of the rhMG53 (or saline) treatment, and these mice do consistently show reduced left ventricular ejection fraction. Our findings are consistent with other published studies showing decreased systolic dysfunction in aged mice (16, 40-42), and rhMG53 treatment had benefits to improve systolic function of the aged mouse heart. Aging is also associated with increased proportion of senescent cells which contribute to inflammation through senescence-associated secretory phenotype production (43). Whether or not rhMG53 could rejuvenate the senescent phenotype of cardiac cells in aging heart remains to be examined in the future.

Two limitations were recognized in this study: First, in addition to the NFkB signal pathway, there might be other pathways involved in the cardiac action of MG53 in age-related heart failure. Therefore, future studies with RNA-seq analysis could be conducted with aging mouse hearts after systemic treatment with rhMG53 to determine the signaling components involved in cardioprotection. Second, while we have data to correlate the reduced MG53 protein expression and cardiac dysfunction in the aging mouse heart, we do not have sufficient number of young, healthy human heart samples to establish if natural aging can also impact the expression of MG53 in healthy human hearts. We have only compared MG53 expression in aged human heart samples from ischemic heart failure to those without heart failure. Future studies with sufficient number of young healthy human heart samples should examine if natural aging impact the expression of MG53 in human heart.

Identification of MG53 as a negative regulator of NFκB, as reflected by the close correlation between reduced MG53 expression and elevated NFκB activation we observed in both human and mouse hearts, shall have broader implications to treatment of other stress-induced heart injuries. For example, the recent outbreak of has caused a devastating global health emergency. While the focus of attention has generally been on the pulmonary manifestations, there is emerging evidence that cardiac involvement may be common (44). Patients infected with SARS-CoV2 have a robust inflammatory response that potentiate the fulminant myocarditis in some patients. Most importantly, cardiac injury occurs more

frequently in elderly patients who suffer from SARC-CoV2 infection and is associated with higher in-hospital mortality (45). While the physiologic base that underlies the susceptible nature of virus-induced dysfunction of the aging heart remains largely unknown, a therapeutic approach such as MG53 that mitigates inflammation and restores cardiomyocyte integrity can potentially be an effective means to treat SARS-CoV2-induced myocarditis in the elderly population. Future studies are required to test whether rhMG53 protein has any therapeutic benefits to treat virus-induced heart injury.

Methods

Experimental animals

Animal handling and surgical procedures were performed according to protocols approved by the Institutional Animal Care and Use Committee (IACUC) of The Ohio State University and were compliant with guidelines of the American Association for the Accreditation of Laboratory Animal Care. The young (3 months) C57BL/6 mice were purchased from Jax lab, and the aging (24-25 months) mice with the C57BL/6 background were obtained from NIA. rhMG53 (6 mg/kg) or saline was subcutaneously injected once a day for a total of 6 weeks. Immediately after the PV-loop measurement, the vital organs, including heart, liver, lung, kidney, and blood serum were collected for further investigation as described below. All experiments were conducted in a blinded fashion, e.g. the person who performed data analysis was only given bar-code labelled animals, heart tissues, and serum samples. Archiving and statistical data analyses were conducted by a third person who has no knowledge of the mouse treatment history.

RNA isolation and quantitative real-time PCR

Real-time qPCR was performed to determine the pro-inflammatory cytokine gene expression, including *IFNγ, IL-1β, IL6,* and *TNFα*, for left ventricle tissue collected from young and aged mice treated with saline or rhMG53. The total RNA of each sample was isolated by using the Rneasy fibrous tissue kit according to the manufacturer's instructions (Qiagen#74704). The reverse transcription of 1ug of RNA to cDNA was performed by using the Bio-Rad iScript cDNA Synthesis kit (Bio-Rad Cat#170-8891). Primer sequences used are: Ifng-F: CTCTTCCTCATGGCTGTTTCT; Ifng-R: TTCTTCCACATCTATGCCACTT; Il1b-F: GGTACATCAGCACCTCACAA; Il1b-R: TTAGAAACAGTCCAGCCCATAC; Il6-F: CTTCCATCCAGTTGCCTTCT; Il6-R: CTCCGACTTGTGAAGTGGTATAG; Tnfa-F: TTGTCTACTCCCAGGTTCTCT; Tnfa-R: GAGGTTGACTTTCTCCTGGTATG. Samples for real-time qPCR were prepared according to the manufacturer's instructions in the iTaq Universal SYBR Green Supermix (Bio-Rad Cat#172-5124), and was run with a Bio-Rad CFX384 Real-Time system.

Immunoblotting

Crude extracts from heart of experimental animals were washed twice with ice-cold PBS and lysed in RIPA buffer (10 mM Tris-HCl, pH 7.2, 150 mM NaCl, 1% NP-40, 0.5% SDS, and 0.5% deoxycolate), supplemented with a cocktail of protease inhibitors (Sigma) and phosphatase inhibitors (Thermo Scientific). Heart lysates were separated by 10% SDS-PAGE and transferred onto polyvinylidene fluoride membranes (PVDF). The blots were washed with Tris-buffered saline Tween-20 (TBST), blocked with 5% milk in TBST for 1 h, and incubated with custom-made monoclonal anti-MG53 antibody(24, 33). Immunoblots were visualized with an ECL plus kit (Pierce). In addition, the following antibodies were used in this study: MG53 (clone 914, home-made) and GAPDH (Sigma); antibodies against p65, and phosphorylated p65 were all purchased from Cell Signaling.

We routinely used multiple samples derived from different animals in a given western blot. To illustrate the spread of the band intensity with the wild type samples, we normalized the band intensity to one control sample (which is often the one with middle intensity) and plotted the relative intensity of other samples in the scatter plot.

Echocardiography

Serial M-mode echocardiographic images of mice subjected to 1-2% isoflurane anesthesia were obtained via Vevo 2100 imaging platform (VisualSonics, Inc. Canada) at baseline (4 days prior to rhMG53 administration), 2 weeks, 4 weeks, and 6 weeks after rhMG53 injection. Using a rectal temperature probe, body temperature was carefully maintained between 36.7 and 37.3 ˚C throughout the study. Hearts were viewed in the short-axis between the two papillary muscles. Each measurement was obtained with M-mode by averaging results from three consecutive heart beats. Left ventricular internal dimensions (LVID) at diastole and systole (LVIDd and LVIDs) were measured. LV ejection fraction (EF) was calculated using the following formula: EF (%) =100× [(LVIDd3 –LVIDs3)/LVIDd3]. Digital images were analyzed off-line by blinded observers using the Vevo 2100 workstation software.

Hemodynamic studies

At week 7 after the first rhMG53 administration, *in vivo* cardiac hemodynamic function was evaluated utilizing the Mikro-Tip® Pressure Volume System (MPVS) Ultra Foundation Systems (AD instruments, Australia) with 1.0 French PVR-1045 micro-tip ultra-miniature pressure–volume (PV) catheter (Millar, Houston, TX). Mice were anesthetized with 1-2% isoflurane, intubated and ventilated with a positive pressure ventilator (Harvard apparatus Minivent Hugo Sachs Electronik, ventilation rate 105/min, tidal volume 10.3 µl/g). Rectal temperature was kept between 36.7 and 37.3 ˚C. The right common carotid artery was isolated and cannulated (PV catheter) for determination of LV performance. The raw pressure and volume data collected in text files by the MPCU-200 unit and Chart/Powerlab software were imported into the PVAN software, which applied a variety of algorithms to the PV data to calculate up to 30 cardiovascular parameters [18, 19]. As in the case of the echo study, all hemodynamic data analyses were performed off-line by investigators blinded to the treatment.

TUNEL staining

At the end of the protocol, the heart was arrested in diastole by an intravenous injection of 0.15 ml of CdCl2 (100 mM), excised, and perfused retrograde at 60–80 mmHg (LVEDP = 8 mmHg) with heparinized PBS followed by 10% neutral buffered formalin solution for 15 min. The heart was then sectioned into three slices from apex to base, fixed in formalin for 24 h, and subjected to tissue processing, paraffin embedding, and heart sectioning. Paraffin-embedded, 4 µm-thick heart sections were deparaffinized in xylene and rehydrated gradually through 100, 95, and 70% ethanol followed by antigen retrieval procedure. After pre-incubation with serum blocking solution, the primary antibodies were applied to identify the expression of different markers, including anti-α actinin (Sarcomeric, SA) and Ab (Sigma, MO) for cardiomyocytes. Terminal deoxynucleotidyltransferase–mediated dUTP nick end labeling (TUNEL) was performed to detect apoptotic nuclei by using terminal deoxynucleotidyltransferase–mediated in situ fluorescein-conjugated dUTP nick end labeling technique according to the

manufacturer's protocol (GeneCopoeia,Inc. MD). Nuclei were counterstained with DAPI. The fluorescence staining was viewed with Zeiss 780 confocal laser-scanning microscope. The number of apoptotic cells with TUNEL-positive nuclei was expressed as a percentage of total cell population.

Dihydroethidium (DHE) fluorescence staining for the *In Situ* detection of ROS production

Frozen heart sections were used to examine the levels of ROS production via DHE fluorescence staining. Briefly, the slices with cross heart sections were first incubated with phosphate-buffered saline (PBS) for 10 minutes at 37°C, then with fresh PBS containing DHE at a final concentration of 5 μM in a light-protected humidified chamber for 30 minutes at 37°C. Images were obtained with a fluorescence microscope (×200 magnification), and the mean fluorescence intensity was quantified by ImageJ.

Blood plasma sample collection and analysis

At the time of sacrificing the mice, whole blood was collected in heparin-treated tubes and centrifuged at 1,000 g for 15 min at 20°C. The upper layer blood plasma was then removed into new tubes for further analysis. The plasma levels of alanine aminotransferase (ALT), alkaline phosphatase (ALP), and total bilirubin (TBILI), high-density lipoprotein (HDL), low density lipoprotein (LDL), triglycerides (TRIG), lactic acid dehydrogenase (LDH), and creatine kinase (CK) were evaluated by Vet Axcel Chemistry Analyzer and liquid ready reagents (Alfa Wassermann Diagnostic Technologies, LLC, US) according to the manufacturer’s protocols.

Statistics

All of the experimental data were analyzed using GraphPad Prism 8.3 software. The standard error of mean (SEM) is indicated by error bars for each group of data. Data were expressed as the mean ± SEM. Comparisons were made by Student’s t-test when comparing two experimental groups. One-way ANOVA followed by Tukey's multiple comparisons test was used to compare data from 3 different groups. A value of $p<0.05$ was considered significant.

Study approval - Human heart samples

Non-failing and failing human patient left ventricular tissues were obtained from donor hearts in collaboration with the Lifeline of Ohio Organ Procurement Program (LOOP). Use of these human tissues were approved by the Institutional Review Board (IRB) of The Ohio State University (Study Number 2012H0197). All participants in these studies were provided with written informed consent. Snap frozen heart tissues were processed in radioimmunoprecipitation assay (RIPA) lysis buffer for western blot analyses.

Author's contribution

X.W. performed the majority of experiments and analyzed the data. X.L., H.O., T.T., K.H.P, Z.B. participated in some of the experiments and data analysis. X.Z., L.C. provided help on the frozen tissue sectioning. E.H., P.J., R.E.M., T.M.P., B.A.W. and N.A.M. provided valuable suggestions to the study. All authors contribute to editing of the manuscript. C.C. and J.M. conceived the study, wrote and revise the manuscript.

Acknowledgments

This work was partially supported by NIH grants (AR061385 and AR070752 to JM, HL153876 to HZ, GM123887 to TT), and AHA grant (18TPA34170188 to CC). We thank the patients and investigators who participated in the Lifeline of Ohio Organ Procurement Program (LOOP) for providing the specimens and clinical data.

References

1. Yang XP, Sreejayan N, and Ren J. Views from within and beyond - Narratives of cardiac contractile dysfunction under senescence. *Endocrine.* 2005;26(2):127-37.
2. Cai C, Masumiya H, Weisleder N, Matsuda N, Nishi M, Hwang M, Ko JK, Lin P, Thornton A, Zhao X, et al. MG53 nucleates assembly of cell membrane repair machinery. *Nat Cell Biol.* 2009;11(1):56-64.
3. Zhu H, Lin P, De G, Choi KH, Takeshima H, Weisleder N, and Ma J. Polymerase transcriptase release factor (PTRF) anchors MG53 protein to cell injury site for initiation of membrane repair. *J Biol Chem.* 2011;286(15):12820-4.
4. Lin P, Zhu H, Cai C, Wang X, Cao C, Xiao R, Pan Z, Weisleder N, Takeshima H, and Ma J. Nonmuscle myosin IIA facilitates vesicle trafficking for MG53-mediated cell membrane repair. *FASEB journal : official publication of the Federation of American Societies for Experimental Biology.* 2012;26(5):1875-83.
5. Liu J, Zhu H, Zheng Y, Xu Z, Li L, Tan T, Park KH, Hou J, Zhang C, Li D, et al. Cardioprotection of recombinant human MG53 protein in a porcine model of ischemia and reperfusion injury. *J Mol Cell Cardiol.* 2015;80(10-9.
6. McNeil P. Membrane repair redux: redox of MG53. *Nature cell biology.* 2009;11(1):7-9.
7. Cao CM, Zhang Y, Weisleder N, Ferrante C, Wang X, Lv F, Zhang Y, Song R, Hwang M, Jin L, et al. MG53 constitutes a primary determinant of cardiac ischemic preconditioning. *Circulation.* 2010;121(23):2565-74.
8. Wang X, Xie W, Zhang Y, Lin P, Han L, Han P, Wang Y, Chen Z, Ji G, Zheng M, et al. Cardioprotection of ischemia/reperfusion injury by cholesterol-dependent MG53-mediated membrane repair. *Circ Res.* 2010;107(1):76-83.
9. Bian Z, Wang Q, Zhou X, Tan T, Park KH, Kramer HF, McDougal A, Laping NJ, Kumar S, Adesanya TMA, et al. Sustained elevation of MG53 in the bloodstream increases tissue regenerative capacity without compromising metabolic function. *Nat Commun.* 2019;10(1):4659.
10. Kohr MJ. Mitsugumin-53: potential biomarker and therapeutic for myocardial ischemic injury? *J Mol Cell Cardiol.* 2015;81(46-8.
11. Gordon JW, Shaw JA, and Kirshenbaum LA. Multiple Facets of NF-kappa B in the Heart To Be or Not to NF-kappa B. *Circ Res.* 2011;108(9):1122-32.
12. Oeckinghaus A, and Ghosh S. The NF-kappaB family of transcription factors and its regulation. *Cold Spring Harbor perspectives in biology.* 2009;1(4):a000034.
13. Helenius M, Hanninen M, Lehtinen SK, and Salminen A. Aging induced up regulation of nuclear binding activities of oxidative stress responsive NF-kB transcription factor in mouse cardiac muscle. *J Mol Cell Cardiol.* 1996;28(3):487-98.
14. Hamid T, Guo SZ, Kingery JR, Xiang XL, Dawn B, and Prabhu SD. Cardiomyocyte NF-kappa B p65 promotes adverse remodelling, apoptosis, and endoplasmic reticulum stress in heart failure. *Cardiovascular research.* 2011;89(1):129-38.
15. Mann DL. Innate Immunity and the Failing Heart The Cytokine Hypothesis Revisited. *Circ Res.* 2015;116(7):1254-68.
16. Dai DF, Chen T, Wanagat J, Laflamme M, Marcinek DJ, Emond MJ, Ngo CP, Prolla TA, and Rabinovitch PS. Age-dependent cardiomyopathy in mitochondrial mutator mice is attenuated by overexpression of catalase targeted to mitochondria. *Aging Cell.* 2010;9(4):536-44.
17. Schulze-Osthoff K, Ferrari D, Los M, Wesselborg S, and Peter ME. Apoptosis signaling by death receptors. *Eur J Biochem.* 1998;254(3):439-59.

18. Hajjar DP, and Gotto AM, Jr. Biological relevance of inflammation and oxidative stress in the pathogenesis of arterial diseases. *The American journal of pathology.* 2013;182(5):1474-81.
19. Feng WJ, Xu XZ, Zhao G, Zhao JJ, Dong RL, Ma B, Zhang YJ, Long GW, Wang DW, and Tu L. Increased Age-Related Cardiac Dysfunction in Bradykinin B2 Receptor-Deficient Mice. *J Gerontol a-Biol.* 2016;71(2):178-87.
20. Guan FX, Zhou XK, Li P, Wang YP, Liu M, Li FF, Cui YB, Huang TJ, Yao MH, Zhang YT, et al. MG53 attenuates lipopolysaccharide-induced neurotoxicity and neuroinflammation via inhibiting TLR4/NF-kappa B pathway in vitro and in vivo. *Prog Neuro-Psychoph.* 2019;95(
21. Liu W, Wang G, Zhang C, Ding W, Cheng W, Luo Y, Wei C, and Liu J. MG53, A Novel Regulator of KChIP2 and Ito,f, Plays a Critical Role in Electrophysiological Remodeling in Cardiac Hypertrophy. *Circulation.* 2019;139(18):2142-56.
22. Sermersheim M, Lin,P, Kenney, A, McMichael, T, Cai, C, Gumpper, K, Adesanya, T.A. , Li, H, Zhou, X, Park, K, Moliva, J, Torelles, J, Yount, J , Ma, J. MG53 Suppresses Interferon-β and Inflammation via Regulation of Ryanodine Receptor-Mediated Intracellular Calcium Signaling. *Nat Commun.* 2020;
23. Lemckert FA, Bournazos A, Eckert DM, Kenzler M, Hawkes JM, Butler TL, Ceely B, North KN, Winlaw DS, Egan JR, et al. Lack of MG53 in human heart precludes utility as a biomarker of myocardial injury or endogenous cardioprotective factor. *Cardiovasc Res.* 2016;110(2):178-87.
24. Adesanya TMA, Russell M, Park KH, Zhou X, Sermersheim MA, Gumpper K, Koenig SN, Tan T, Whitson BA, Janssen PML, et al. MG 53 Protein Protects Aortic Valve Interstitial Cells From Membrane Injury and Fibrocalcific Remodeling. *J Am Heart Assoc.* 2019;8(4):e009960.
25. Wang Q, Bian Z, Jiang Q, Wang X, Zhou X, Park KH, Hsueh W, Whitson BA, Haggard E, Li H, et al. MG53 Does Not Manifest the Development of Diabetes in db/db Mice. *Diabetes.* 2020;69(5):1052-64.
26. Song R, Peng W, Zhang Y, Lv F, Wu HK, Guo J, Cao Y, Pi Y, Zhang X, Jin L, et al. Central role of E3 ubiquitin ligase MG53 in insulin resistance and metabolic disorders. *Nature.* 2013;494(7437):375-9.
27. Tamemoto H, Kadowaki T, Tobe K, Yagi T, Sakura H, Hayakawa T, Terauchi Y, Ueki K, Kaburagi Y, Satoh S, et al. Insulin resistance and growth retardation in mice lacking insulin receptor substrate-1. *Nature.* 1994;372(6502):182-6.
28. Terauchi Y, Iwamoto K, Tamemoto H, Komeda K, Ishii C, Kanazawa Y, Asanuma N, Aizawa T, Akanuma Y, Yasuda K, et al. Development of non-insulin-dependent diabetes mellitus in the double knockout mice with disruption of insulin receptor substrate-1 and beta cell glucokinase genes. Genetic reconstitution of diabetes as a polygenic disease. *The Journal of clinical investigation.* 1997;99(5):861-6.
29. Wu HK, Zhang Y, Cao CM, Hu X, Fang M, Yao Y, Jin L, Chen G, Jiang P, Zhang S, et al. Glucose-Sensitive Myokine/Cardiokine MG53 Regulates Systemic Insulin Response and Metabolic Homeostasis. *Circulation.* 2019;139(7):901-14.
30. Zhu H, Hsueh W, and Whitson BA. Letter by Zhu et al Regarding Article, "Glucose-Sensitive Myokine/Cardiokine MG53 Regulates Systemic Insulin Response and Metabolic Homeostasis". *Circulation.* 2019;140(6):e186-e7.
31. Weisleder N, Takizawa N, Lin P, Wang X, Cao C, Zhang Y, Tan T, Ferrante C, Zhu H, Chen PJ, et al. Recombinant MG53 protein modulates therapeutic cell membrane repair in treatment of muscular dystrophy. *Sci Transl Med.* 2012;4(139):139ra85.
32. Jia Y, Chen K, Lin P, Lieber G, Nishi M, Yan R, Wang Z, Yao Y, Li Y, Whitson BA, et al. Treatment of acute lung injury by targeting MG53-mediated cell membrane repair. *Nat Commun.* 2014;5(4387.

33. Duann P, Li H, Lin P, Tan T, Wang Z, Chen K, Zhou X, Gumpper K, Zhu H, Ludwig T, et al. MG53-mediated cell membrane repair protects against acute kidney injury. *Sci Transl Med.* 2015;7(279):279ra36.

34. Guan F, Huang T, Wang X, Xing Q, Gumpper K, Li P, Song J, Tan T, Yang GL, Zang X, et al. The TRIM protein Mitsugumin 53 enhances survival and therapeutic efficacy of stem cells in murine traumatic brain injury. *Stem cell research & therapy.* 2019;10(1):352.

35. Morishita R, Sugimoto T, Aoki M, Kida I, Tomita N, Moriguchi A, Maeda K, Sawa Y, Kaneda Y, Higaki J, et al. In vivo transfection of cis element "decoy" against nuclear factor-kappaB binding site prevents myocardial infarction. *Nat Med.* 1997;3(8):894-9.

36. Derumeaux G, Ichinose F, Raher MJ, Morgan JG, Coman T, Lee C, Cuesta JM, Thibault H, Bloch KD, Picard MH, et al. Myocardial alterations in senescent mice and effect of exercise training: a strain rate imaging study. *Circulation Cardiovascular imaging.* 2008;1(3):227-34.

37. Kiermayer C, Northrup E, Schrewe A, Walch A, de Angelis MH, Schoensiegel F, Zischka H, Prehn C, Adamski J, Bekeredjian R, et al. Heart-Specific Knockout of the Mitochondrial Thioredoxin Reductase (Txnrd2) Induces Metabolic and Contractile Dysfunction in the Aging Myocardium. *Journal of the American Heart Association.* 2015;4(7).

38. Kuppuswamy D, Chinnakkannu P, Reese C, and Hoffman S. The Caveolin-1 Scaffolding Domain Peptide Reverses Aging-Associated Deleterious Changes in Multiple Organs. *The Journal of pharmacology and experimental therapeutics.* 2021.

39. Li X, Liu J, Hu H, Lu S, Lu Q, Quan N, Rousselle T, Patel MS, and Li J. Dichloroacetate Ameliorates Cardiac Dysfunction Caused by Ischemic Insults Through AMPK Signal Pathway-Not Only Shifts Metabolism. *Toxicological sciences : an official journal of the Society of Toxicology.* 2019;167(2):604-17.

40. Boyle AJ, Shih H, Hwang J, Ye JQ, Lee B, Zhang Y, Kwon D, Jun K, Zheng DW, Sievers R, et al. Cardiomyopathy of aging in the mammalian heart is characterized by myocardial hypertrophy, fibrosis and a predisposition towards cardiomyocyte apoptosis and autophagy. *Exp Gerontol.* 2011;46(7):549-59.

41. Koonen DP, Febbraio M, Bonnet S, Nagendran J, Young ME, Michelakis ED, and Dyck JR. CD36 expression contributes to age-induced cardiomyopathy in mice. *Circulation.* 2007;116(19):2139-47.

42. Medrano G, Hermosillo-Rodriguez J, Pham T, Granillo A, Hartley CJ, Reddy A, Osuna PM, Entman ML, and Taffet GE. Left Atrial Volume and Pulmonary Artery Diameter Are Noninvasive Measures of Age-Related Diastolic Dysfunction in Mice. *The journals of gerontology Series A, Biological sciences and medical sciences.* 2016;71(9):1141-50.

43. Anderson R, Lagnado A, Maggiorani D, Walaszczyk A, Dookun E, Chapman J, Birch J, Salmonowicz H, Ogrodnik M, Jurk D, et al. Length-independent telomere damage drives post-mitotic cardiomyocyte senescence. *Embo J.* 2019;38(5).

44. Driggin E, Madhavan MV, Bikdeli B, Chuich T, Laracy J, Bondi-Zoccai G, Brown TS, Nigoghossian C, Zidar DA, Haythe J, et al. Cardiovascular Considerations for Patients, Health Care Workers, and Health Systems During the Coronavirus Disease 2019 (COVID-19) Pandemic. *Journal of the American College of Cardiology.* 2020.

45. Shi S, Qin M, Shen B, Cai Y, Liu T, Yang F, Gong W, Liu X, Liang J, Zhao Q, et al. Association of Cardiac Injury With Mortality in Hospitalized Patients With COVID-19 in Wuhan, China. *JAMA cardiology.* 2020.

Figures and Figure legends

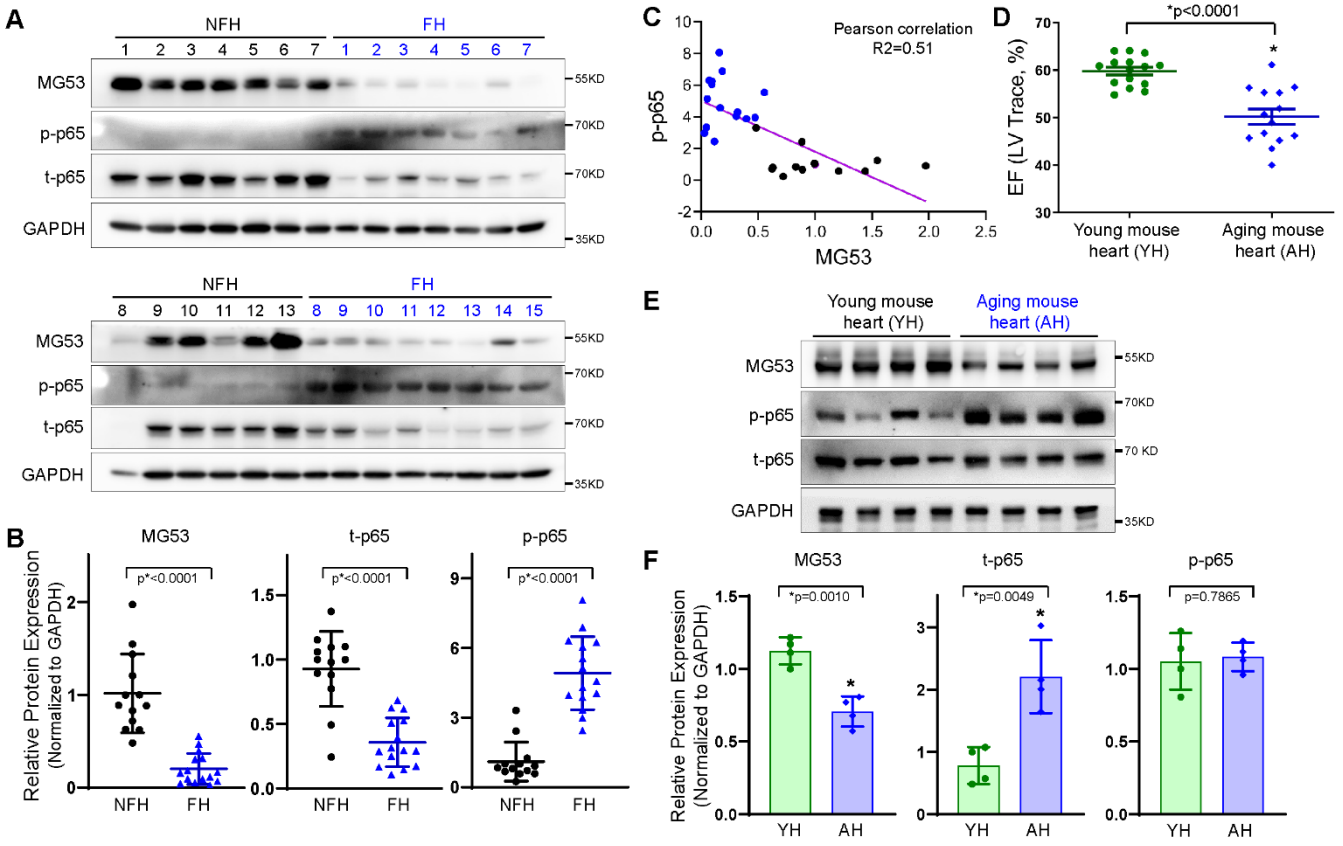

Figure 1. Failing human hearts and aging mouse hearts show reduced MG53 and increased p65 activation. (A) Western blot of MG53, total p65 (t-p65) and phosphorylated p65 (p-p65) in non-failing human hearts (NFHs, n=13) and failing human hearts (FHs, n=15). GAPDH serves as loading control. **(B)** Quantification of MG53, t-p65, and p-p65 in NFH and HF tissues. **(C)** Inverse correlation between MG53 and p-p65 expression in human heart tissues. **(D)** Left ventricle EF for young (3 months, n=15) and aging (24 months, n=14) mouse. **(E)** Western blot for MG53, p-p65, p65 in young mouse hearts (YH, 3 months, n=4) and aging (AH, 24 months, n=4) mouse hearts. **(F)** Quantification of MG53, t-p65, and p-p65 expression in young and aging mouse hearts. Data are expressed as mean ± SEM. Statistics differences were analyzed by unpaired *t* test. P values are presented in the individual panels.

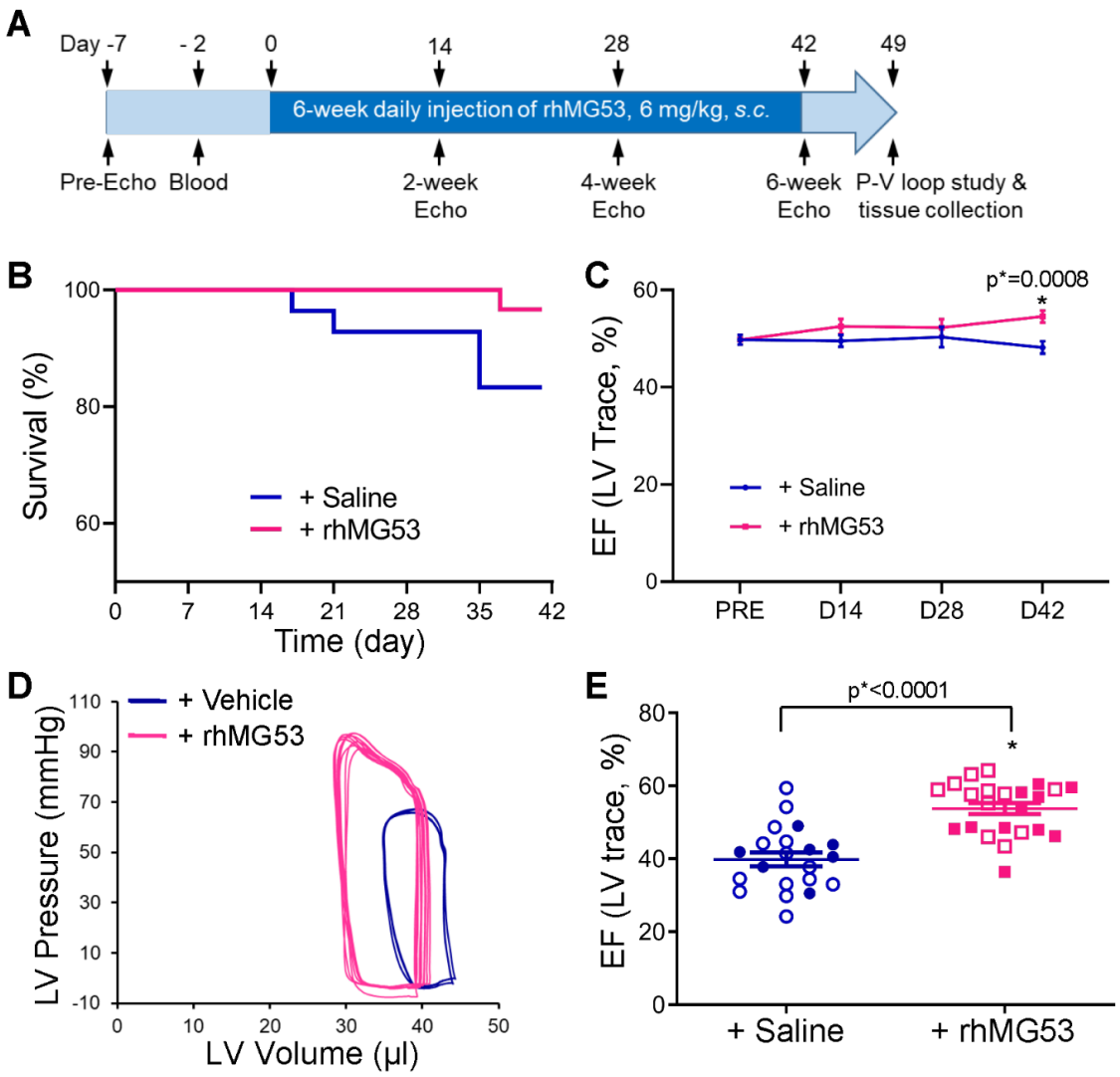

Figure 2. Systematic administration of rhMG53 mitigates HF in aging mice. (A) Schematic protocol for the 6-week daily administration of rhMG53 in aging mouse. **(B)** Survival curve for mice with systematic administration of rhMG53 (n=30) or saline control (n=30). 15 male and 15 female mice per group. **(C)** Longitudinal echocardiography measurements of aged mice with saline and rhMG53 treatments. **(D)** Representative pressure-volume loop for the assessment of aged mouse heart function after treatment with saline or rhMG53. **(E)** Quantitative analysis of the left ventricle EF for the PV-loop measurements for mice treated with saline and rhMG53. Open symbols - male mice; closed symbols - female mice. Data are expressed as mean ± SEM. Statistics differences were analyzed by unpaired *t* test (**C** and **E**). P values are presented in the individual panels.

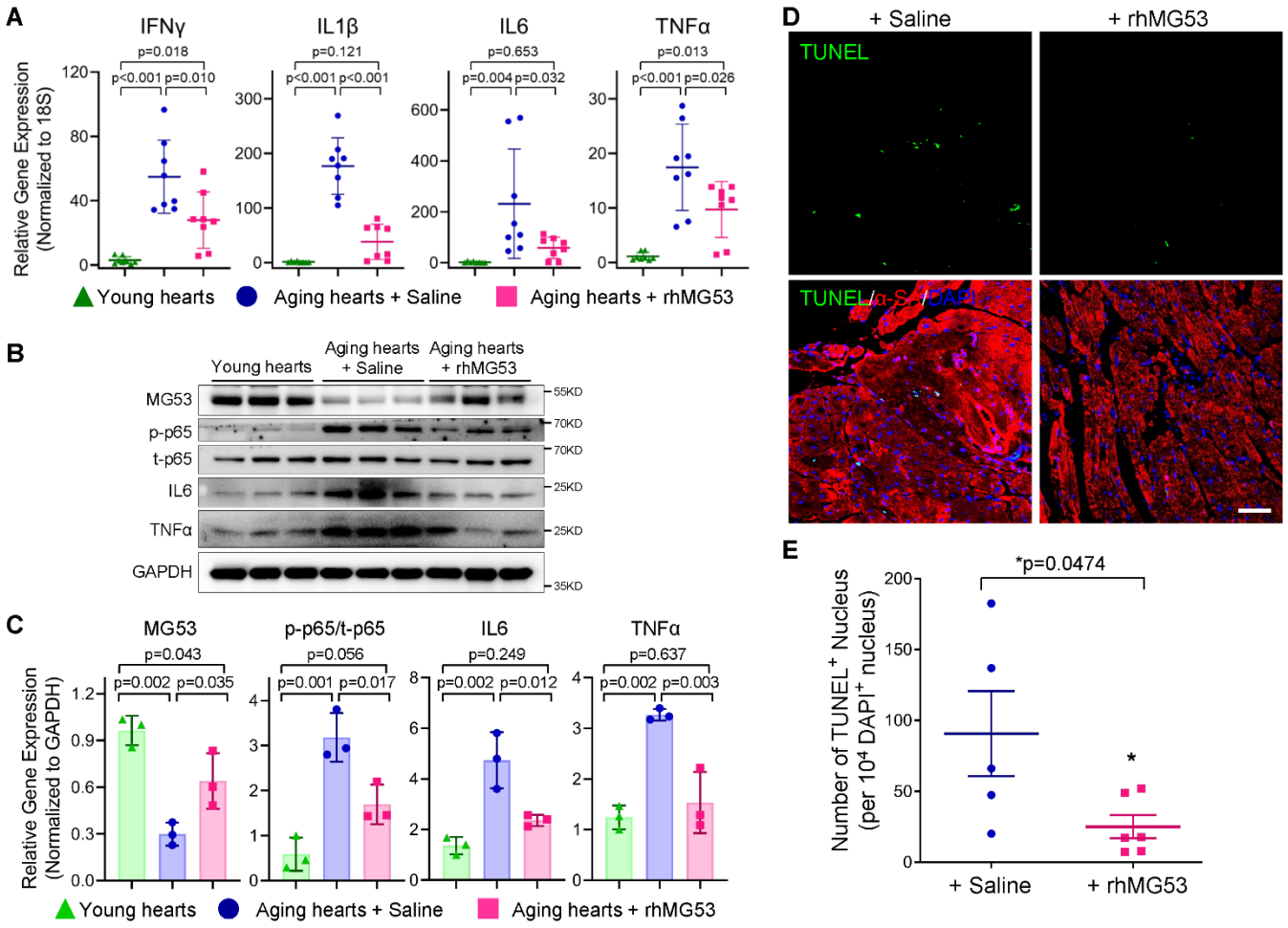

Figure 3. Longitudinal treatment with rhMG53 suppress the activation of NFκB signal pathway and the cardiac cell death. **(A)** Quantitative real-time PCR analysis showed the relative mRNA expression of pro-inflammatory marker genes, including *IFNγ, IL1β, IL6, TNFα*, in cardiac muscle collected from young mice (YH, 3 months), aging mice treated with saline or rhMG53 (AH, 25.5 months) aging mice treated with or without rhMG53 (n=8 per group). **(B-C)** Western blot and quantitative analysis of MG53, phosphorylated and total p65, IL6, TNFα, and GAPDH as the loading control in heart tissues derived from young mice, and aging mice treated with saline or rhMG53, n=3. **(D-E)** Representative confocal images and quantitative analysis for the TUNEL staining of heart sections from aged mice treated with rhMG53 (n=6) or saline (n=5). Bar = 100 μm. Data are expressed as mean ± SEM. P values calculated using one-way ANOVA with Tukey's multiple-comparison test (**A** and **C**), or unpaired *t* test (**E**). P values are presented in the individual panels.

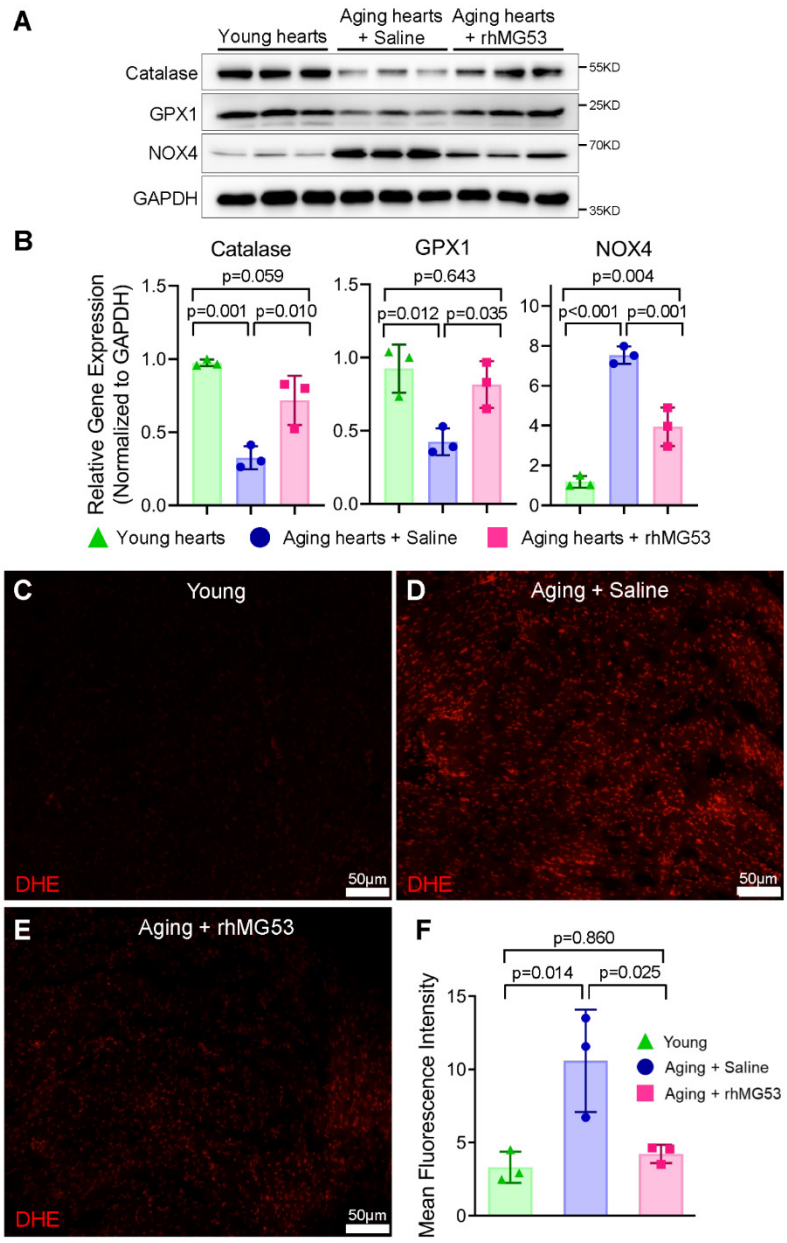

Figure 4. Daily administration of rhMG53 regulated the expression of oxidative stress associated proteins and suppress the age-related reactive oxygen species (ROS) generation. **(A-B)** Western blot and quantitative analysis of catalase, GPX1, NOX4, and GAPDH as the loading control in heart tissues derived young mice (3 months), aging mice treated with saline or rhMG53 (25.5 months). The samples and loading condition were identical to Fig. 3B. **(C-E)** Cross-sections of mouse left ventricles stained with dihydroethidium (DHE) for quantification of ROS in young mice (**C**), and aging mice treated with saline (**D**) or rhMG53 (**E**), n=3. **(F)** The quantitative data of **C-E**. Data are expressed as mean ± SEM. P values calculated using one-way ANOVA with Tukey's multiple-comparison test (**B** and **F**). P values are presented in the individual panels.

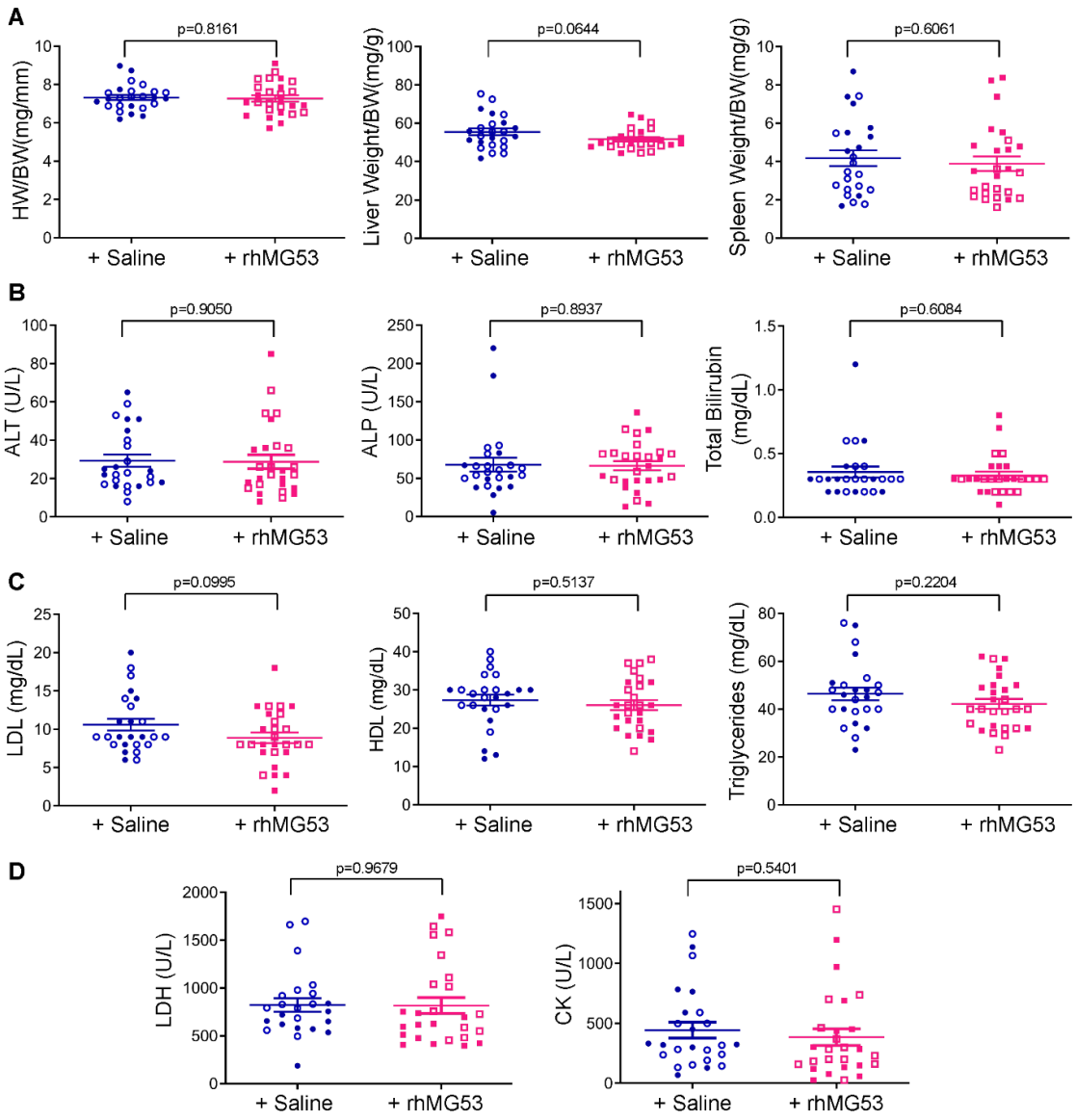

1 **Figure 5. Repetitive administration of rhMG53 is safe in aging mice**. **(A)** The ratios of heart
2 weight/tibia length (HW/TL), liver weight/body weight (BW) and spleen weight/BW were not significantly
3 changed after 6-weeks administration of rhMG53 in aging mice versus the saline group. **(B)** Serum levels
4 of ALT, ALP, and bilirubin in mice treated with saline or rhMG53. **(C)** Serum levels of LDL, HDL, and
5 triglycerides in mice treated with saline or rhMG53. **(D)** Serum levels of LDH and CK in mice treated with
6 saline or rhMG53. Open symbols - male mice; closed symbols - female mice. Data are expressed as
7 mean ± SEM. Statistics differences were analyzed by unpaired *t* test (**A-D**). P values are presented in
8 the individual panels.

Table 1. The demographic information of the human patients without failing heart (NFH) or with failing heart (FH).

Label	Internal ID	Age	Gender	Disease type
NFH-1	156910	62	F	NFH
NFH-2	727865	67	F	NFH
NFH-3	507207	72	F	NFH
NFH-4	957855	63	M	NFH
NFH-5	645817	71	M	NFH
NFH-6	442404	69	M	NFH
NFH-7	674541	64	M	NFH
NFH-8	947200	63	F	NFH
NFH-9	460025	69	F	NFH
NFH-10	632941	68	F	NFH
NFH-11	481043	65	F	NFH
NFH-12	574165	62	M	NFH
NFH-13	749693	65	M	NFH
FH-1	525466	68	M	Ischemic HF
FH-2	335581	70	M	Ischemic HF
FH-3	142599	62	M	Ischemic HF
FH-4	851358	68	M	Ischemic HF
FH-5	120402	68	F	Ischemic HF
FH-6	120524	61	M	Ischemic HF
FH-7	120728	61	F	Ischemic HF
FH-8	328163	63	M	Ischemic HF
FH-9	142602	68	F	Ischemic HF
FH-10	537263	62	M	Ischemic HF
FH-11	214010	64	M	Ischemic HF
FH-12	597750	67	M	Ischemic HF
FH-13	514955	67	F	Ischemic HF
FH-14	233587	65	M	Ischemic HF
FH-15	250585	65	M	Ischemic HF